Alqalam Journal of Medical and Applied Sciences. 2026;9(5):1184-1204
https://doi.org/10.54361/ajmas.269509

Original article

Targeted Cytotoxicity and Docking Studies of Novel Benzenesulfonamide Derivatives Against Human Cancer Cell Lines

Hussniya AlDifar*, Basma Baaiu, Fakhri Elabbar

Department of Chemistry, Faculty of Science, Benghazi, University of Benghazi, P.O. Box 1308, Benghazi, Libya.
Corresponding Email. *Hussnya.difar@uob.edu.ly*

Abstract
This study investigates the synthesis and cytotoxicity of four novel benzene sulfonamide derivatives (5a-d) derived from enaminone and sulfa drugs, assessed against human cell lines WI-38, MCF-7, HePG-2, and HCT-116, utilizing the MTT assay with doxorubicin and sorafenib as controls. Different IC_{50} values showed that the compounds had different cytotoxic profiles. For example, compound 5d was very effective in MCF-7 (IC_{50} = 31.93 ± 2.2 µM), but compound 5d was less effective in HCT-116 (IC_{50} = 38.44 ± 2.3 µM). These findings on the tumor microenvironment propose that structural alterations may augment anticancer efficacy. Also, when the synthesized compounds were docked against doxorubicin, it was found that compounds 5a and 5b had the strongest binding affinities in MCF-7 (-12.1 and -12.0 kcal/mol, respectively). Compounds 5a and 5b established numerous hydrogen bonds, thereby increasing binding stability, Wears compound 5d demonstrated diminished interactions. These results make people more aware of these compounds as possible treatments for cancer.
Keywords. Enaminone, Cytotoxic, MCF-7, HePG-2, HCT116.

Introduction

Cancer is a major global health concern, identified by rapid cell growth and significant mortality rates [1,2]. Breast cancer is particularly prominent among cancer types, especially affecting women more than men. About 60% of breast cancer instances are hormone-sensitive subtypes, focusing on those that have estrogen receptor beta (ERβ) [3,4]. More over, triple-negative breast cancer (TNBC), characterized by a lack of ERα, progesterone receptor (PR), and HER2, creates additional difficulties for treatment due to its tendency to resist conventional therapies [5,6].

Projections suggest that cancer could soon overtake heart disease as the primary global cause of death, as evidenced by 2018 statistics showing 18 million new cases and 9.6 million deaths [7]. While advancements in treatment approaches have been made, challenges like drug resistance and adverse effects emphasize the urgent need for innovative and targeted cancer treatments [8,9]. Heterocyclic compounds, particularly those with sulfonamide groups, play a crucial role because of their broad biological activities, including antimicrobial, anti-inflammatory, and anticancer properties [10,11]. By serving as bioisosteres for carboxylic groups, sulfonamides may enhance metabolic stability and reduce toxicity [12,13]. Notable treatments such as Belinostat and ABT-199 have been approved for cancer therapy, targeting pathways like histone deacetylase (HDAC) and Bcl-2 [14,15]. Still, it is essential to recognize that sulfonamides may lead to side effects, which can range from gastrointestinal issues to serious allergic reactions like Stevens-Johnson syndrome, notably in compounds containing aromatic amine groups [16,17]. Regardless, drugs such as sulfamethazine (SMZ) and sulfadiazine (SDZ) remain widely used in both human and veterinary medicine [10,18].

Recent research has expanded sulfonamides' therapeutic roles by linking them with heterocyclic frameworks like triazine, isoxazole, and pyrimidine. These combination compounds demonstrate enhanced drug qualities, particularly in their anticancer effectiveness [19]. For instance, hybrids of sulfonamide and triazine have shown strong cytotoxic activity against a variety of cancer cell lines, often surpassing traditional medications like doxorubicin (DOX) in some scenarios [19]. Similarly, sulfonamide-isoxazole and sulfonamide-pyrimidine hybrids show considerable growth inhibition in colon (HCT-116) and liver (HePG-2) cancer cells, highlighting their therapeutic promise [19]. Benzofuran derivatives represent another vital type of heterocyclic compound, recognized for their diverse pharmacological benefits, such as anticancer, antimicrobial, anti-inflammatory, and antiviral effects [20,21].

Naturally occurring benzofurans like angelicin and psoralen, along with synthetic variants such as Amiodarone and Bufuralol, underscore their clinical importance [22, 23]. Recent investigations have found that benzofuran derivatives can be notably toxic to lung cancer cell lines (A549, NCI-H460), achieving IC50 values that rival or exceed those of conventional therapies [24, 25]. Enhancing anticancer efficacy frequently involves structural modifications, such as incorporating ester or heterocyclic groups [23]. Additionally, hybrids like benzofuran-1,3,4-oxadiazole and benzofuran-chalcone conjugates exhibit promising prospects in targeting oncogenic pathways, including PI3K/AKT and EGFR-TK, and may help combat multidrug resistance (MDR) in non-small cell lung cancer (NSCLC) [26, 27]. Benzenesulfonamide has become notable as a substance because of its function as an anticancer drug [28-33] (Figure 1).

Received*: 03-03-2026 -* ***Accepted****: 01-05-2026 -* ***Published****: 09-05-2026*

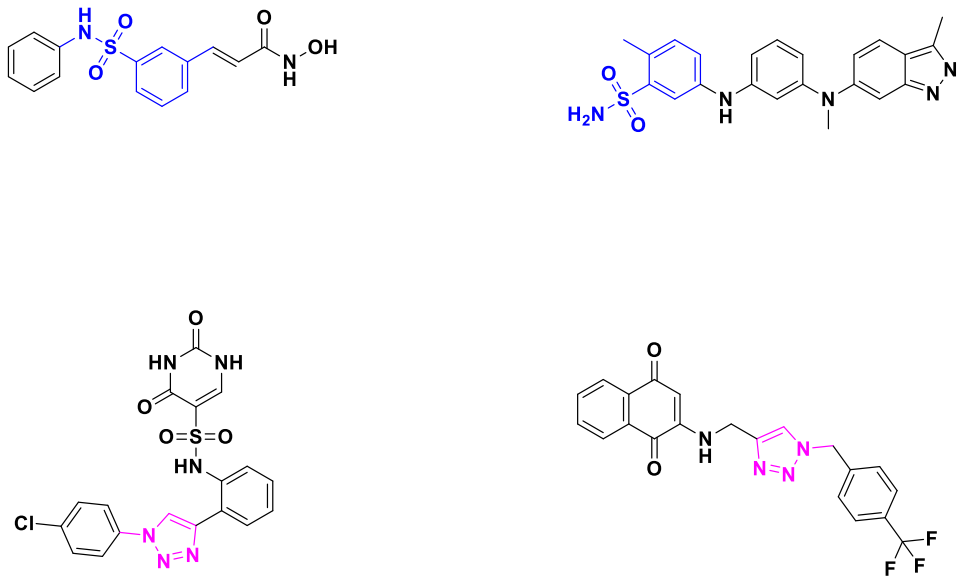

Figure 1. Anticancer benzenesulfonamide derivatives

Methods

Chemistry

General Procedures

Melting points were measured on an electrothermal digital apparatus. IR spectra (KBr disks) were recorded on a Shimadzu FT-IR 8201 PC Infrared spectrophotometer. ^{1}H NMR spectra were recorded in DMSO-d_6 solutions on a Bruker spectrometer operating at 400 MHz, ^{13}CNMR were recorded on a Bruker spectrometer at 100 MHz, and chemical shifts were referenced to that of the solvent.

Synthesis of (E)-3-(dimethylamino)-1-(5-nitrobenzofuran-2-yl) prop-2-en-1-one (3)

A mixture of 1-(5-nitrobenzofuran-2-yl) ethan-1-one (2 g, 10 mmol) and DMF-DMA (1.19 g, 10 mmol) in dry xylene (30 mL) was heated under reflux for 3 hours. After boiling, the solvent was removed, and the residue was triturated with petroleum ether (40–60°C). The obtained solid was collected and purified by recrystallization from ethanol, yielding pink crystals (78% yield). M.p. 242–244°C (dioxane); FT-IR (KBr) ν cm^{-1}: 3074 (HC, aromatic), 1692 (C=C), 1643 (C=O); H NMR (400 MHz, DMSO-d_6): δ 7.97 (d, J = 1.7 Hz, 1H, benzofuran-CH), 7.93 (s, 1H, benzofuran-CH), 7.86 (d, J = 1.7 Hz, 1H, benzofuran-CH), 7.83 (d, J = 12.4 Hz, 1H, =CH–N), 7.62 (s, 1H, benzofuran-CH), 5.79 (d, J = 12.4 Hz, 1H, =CH–CO), 3.20 (s, 3H, CH_3), 2.95 (s, 3H, CH_3); ^{13}CNMR(100 MHz, DMSO-d_6): δ 27.1 (one signal reported; full data missing in original). Anal. Calculated for $C_{13}H_{12}N_2O_4$ (260.25): C, 60.00; H, 4.65; N, 10.76. Found: C, 59.08; H, 4.60; N, 10.70.

General Procedure for the Synthesis of Compounds 5a–d

A mixture of enaminone 3 (0.260 g, 1 mmol), the respective sulfa drug 4a–d (1 mmol each), and a few drops of acetic acid was heated. During this time, a color change (colorless → pink → brown) occurred. After completion of the reaction (monitored by TLC), the mixture was poured into water. The solid product was filtered, washed with ethanol, dried, and recrystallized from DMF to afford compounds 5a–d, respectively. The physical constants of products 5a–d are listed below.

(E)-N-(3,4-dimethylisoxazol-5-yl)-4-((3-(5-nitrobenzofuran-2-yl)-3-oxoprop-1-en-1-yl) amino) benzenesulfonamide (5a)

Dark pink solid, yield 87%. M.p. 320–322°C (DMF); FT-IR (KBr) ν cm^{-1}: 3394 (NH), 3055 (CH, aromatic), 2923 (CH), 1684 (C=C), 1642 (C=O), 1588 (C=N); ^{1}H NMR (400 MHz, DMSO-d_6): δ 8.83 (s, 1H, NH), 8.52 (d, J = 2.6 Hz, 1H, benzofuran-CH), 8.45 (s, 1H, NH), 8.40 (dd, J = 9.2, 2.2 Hz, 1H, benzofuran-CH), 8.06 (s, 1H, C–H furan), 8.01 (d, J = 9.1 Hz, 1H, benzofuran-CH), 7.75 (d, J = 8.6 Hz, 1H, =CH–N), 7.11 (d, J = 9.0 Hz, 2H, aromatic), 7.03 (d, J = 9.1 Hz, 2H, aromatic), 6.57 (d, J = 8.7 Hz, 1H, =CH–CO), 2.33 (s, 3H, CH_3), 1.92 (s, 3H, CH_3); 13CNMR (100 MHz, DMSO-d_6): δ 111.50, 112.47, 113.73, 115.77, 116.98, 117.87, 120.87, 121.53, 121.89, 122.57, 123.55, 126.41, 128.07, 130.07, 130.67, 153.40, 156.05, 157.23, 158.24, 165.38, 172.53, 178.92. Anal. Calculated for $C_{22}H_{18}N_4O_7S$ (482.47): C, 54.77; H, 3.76; N, 11.61; S, 6.65. Found: C, 54.70; H, 3.70; N, 11.60; S, 6.60.

Received*: 03-03-2026 -* ***Accepted****: 01-05-2026 -* ***Published****: 09-05-2026*

(E)-N-(4,6-dimethylpyrimidin-2-yl)-4-((3-(5-nitrobenzofuran-2-yl)-3-oxoprop-1-en-1-yl) amino) benzenesulfonamide (5b)

Brown solid, yield 77%. M.p. 249–251°C (DMF); FT-IR (KBr) ν cm^{-1}: 3264 (NH), 3056 (CH, aromatic), 2937 (CH), 1677 (C=O), 1597 (C=N); ^{1}H NMR (400 MHz, DMSO-d_6): δ 8.77 (s, 1H, NH), 8.71 (d, J = 2.6 Hz, 1H, benzofuran-CH), 8.40 (s, 1H, NH), 8.35 (dd, J = 9.1, 2.6 Hz, 1H, benzofuran-CH), 8.00 (s, 1H, C–H furan), 7.96 (d, J = 9.1 Hz, 2H, aromatic), 7.71 (d, J = 9.2 Hz, 1H, benzofuran-CH), 7.35 (d, J = 8.7 Hz, 1H, =CH–N), 6.99 (d, J = 9.2 Hz, 2H, aromatic), 6.57 (s, 1H, pyrimidine-CH); ^{13}CNMR(100 MHz, DMSO-d_6): δ 113.87, 115.65, 118.05, 120.83, 121.86, 122.32, 123.98, 125.81, 138.72, 138.93, 144.78, 156.08, 158.22, 158.24, 165.98, 172.53, 178.92. Anal. Calculated for $C_{23}H_{19}N_5O_6S$ (493.49): C, 55.98; H, 3.88; N, 14.19; S, 6.50. Found: C, 55.80; H, 3.85; N, 14.15; S, 6.45.

(E)-4-((3-(5-Nitrobenzofuran-2-yl)-3-oxoprop-1-en-1-yl) amino)-N-(1H-1,2,3-triazol-5-yl) benzenesulfonamide (5c)

Pink solid, yield 85%. M.p. 239–241°C (DMF); FT-IR (KBr) ν cm^{-1}: 3585, 3381 (NH_2), 3235 (NH), 3095 (CH, aromatic), 2815 (=CH), 1684 (C=C), 1631 (C=O); ^{1}H NMR (400 MHz, DMSO-d_6): δ 10.17 (s, 1H, NH), 8.80 (s, 1H, NH), 8.59 (d, J = 2.3 Hz, 1H, benzofuran-CH), 8.38 (d, J = 9.1 Hz, 1H, benzofuran-CH), 8.30 (s, 1H, C–H furan), 8.23 (dd, J = 9.2, 2.4 Hz, 1H, benzofuran-CH), 7.83 (d, J = 8.2 Hz, 2H, aromatic), 7.45 (d, J = 8.3 Hz, 2H, aromatic), 7.38 (d, J = 8.5 Hz, 1H, =CH–CO), 5.94 (s, 4H, NH_2). Anal. Calculated for $C_{17}H_{16}N_6O_6S$ (432.41): C, 47.22; H, 3.73; N, 19.44; S, 7.41. Found: C, 47.20; H, 3.70; N, 19.40; S, 7.38.

(E)-N-(4-aminophenyl)-4-((3-(5-nitrobenzofuran-2-yl)-3-oxoprop-1-en-1-yl) amino) benzenesulfonamide (5d)

Pink solid, yield 70%. M.p. 250–252°C (DMF); FT-IR (KBr) ν cm^{-1}: 3477, 3374 (NH_2), 3263 (NH), 3095 (CH, aromatic), 2673 (=CH), 1697 (C=C), 1629 (C=O); ^{1}H NMR (400 MHz, DMSO-d_6): δ 10.31 (s, 1H, NH), 8.80 (s, 1H, NH), 8.42 (d, J = 2.3 Hz, 1H, benzofuran-CH), 8.38 (d, J = 9.1 Hz, 1H, benzofuran-CH), 7.96 (s, 1H, C–H furan), 7.85 (dd, J = 9.1, 2.3 Hz, 1H, benzofuran-CH), 7.74 (s, 2H, aromatic), 7.45 (d, J = 8.4 Hz, 1H, =CH–N), 6.90 (s, 2H, aromatic), 6.59 (d, J = 8.4 Hz, 1H, =CH–CO), 5.83 (s, 2H, NH_2). Anal. Calculated for $C_{23}H_{18}N_4O_6S$ (478.48): C, 57.74; H, 3.79; N, 11.71; S, 6.70. Found: C, 57.70; H, 3.75.

Cytotoxicity assay

Cell line

The cell lines WI-38, MCF-7, HePG-2, and HC116 were purchased from American Type Culture Collection (ATCC, Manassas, VA, USA). Doxorubicin and sorafenib were used as standard anticancer drugs.

Cell Culture

The inhibitory effects of novel synthesized benzenesulfonamide derivatives (5a-d) on the growth of WI-38, MCF-7, HePG-2, and HCT116 cell lines were assessed using the MTT assay. The cells were cultured in 100 mm plates (Sarstedt, Newton, NC, USA) in RPMI-1640 medium (Sigma, St. Louis, USA) supplemented with 10% fetal bovine serum (GIBCO, UK) and antibiotics (penicillin at 100 units/ml and streptomycin at 100 µg/ml). They were incubated under optimal growth conditions (5% CO_2, 37°C, and 90–95% humidity). Following this, the cells were seeded in a 96-well plate at a density of 1.0 x 10^4 cells/well and incubated at 37°C for 48 hours in a 5% CO_2 atmosphere [38].

Cell Viability Assay

The effects of novel synthesized benzenesulfonamide derivatives 5a-d on selected cell lines (WI-38, MCF-7, HePG-2, and HCT116) were evaluated using the MTT assay, following previously described methods [39-41]. After incubation, the cells were treated with varying concentrations of the compounds (1.56, 3.125, 6.25, 12.5, 25, 50, and 100 µM) and incubated for 24 hours. Following this treatment, 20 µl of MTT solution (5 mg/ml) was added to each well and incubated for an additional 4 hours. The resulting purple formazan crystals were dissolved by adding 100 µl of DMSO to each well. The absorbance was measured at 570 nm using a plate reader (EXL 800, USA). Relative cell viability was calculated as follows: (A570 of treated samples / A570 of untreated samples) × 100.

Molecular Docking Studies

Molecular docking studies were conducted using AutoDock Vina version 1.1.2 (released May 11, 2011), with grid dimensions set to 60 × 60 × 60 Å and a grid spacing of 0.375 Å. The run parameters included an exhaustiveness of 32 and a maximum of 100 modes. All synthesized compounds were optimized as 3D structures using Avogadro software (version 1.2.0), with energy minimization performed under the MMFF94s force field for 10,000 steps. The compounds were prepared as ligands using AutoDock Tool version 1.5.7, where Gasteiger charges were assigned, non-polar hydrogens were added, and torsions were specified. The files were then saved in PDBQT format. Doxorubicin, used as a reference drug, was prepared using the same procedure. Crystal structures of the target proteins were downloaded from the PDB repository (https://www.rcsb.org) for MCF-7 (PDB ID: 4XO6), HePG-2 (PDB ID: 5EQG), and HCT116 (PDB ID: 1DI8).

Received*: 03-03-2026 -* ***Accepted****: 01-05-2026 -* ***Published****: 09-05-2026*

All proteins were prepared with AutoDock Tool and saved as PDBQT format files. The docking calculations were performed using AutoDock Vina, and the docking procedure was validated by re-docking the co-crystalized ligand with the target receptor. Visualizations of ligand-protein interactions were carried out using BIOVIA Discovery Studio version 24.1.0.

Results and Discussion

Chemistry

Reaction of 1-(5-nitrobenzofuran-2-yl) ethan-1-one compound 1 with dimethylformamide dimethyl acetal in dry xylene afforded enaminone compound 3. The structure was confirmed by spectral data; the IR spectrum showed an absorption band at 1692 cm^{-1} attributed to the C=C bond, a broad band at 1643 cm^{-1} corresponding to the carbonyl group. The ^{1}HNMR spectrum of such a product revealed two singlets at δ 2.95 and 3.20 corresponding to *N, N-dimethylamino protons*, two doublets at δ 5.79 and 7.83 (J = 12.4 Hz) corresponding to ethylenic protons, in addition to three signals at δ 7.97, 7.93, and 7.86 due to benzofuran protons. On the basis of the coupling constant value for the olefinic protons, the enaminone 3 exists most likely in the *E*-configuration (scheme 1).

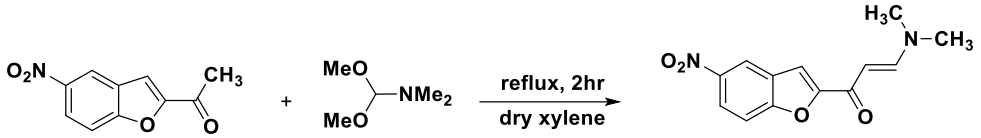

1 2 3

Scheme 1. Synthesis of (E)-3-(dimethylamino)-1-(5-nitrobenzofuran-2-yl) prop-2-en-1-one (3)

Reaction of enaminone 3 with appropriate benzenesulfonamide derivatives 4a-d produced compounds 5a-d (scheme 2). The reaction mechanism outlined in (Scheme 3) [34,35]. The structures of synthesized compounds were confirmed by spectral data, thus the IR spectrum demonstrated absorption bands in the range of 3235–3394 cm^{-1}, suggesting the presence of a H-N bond, bands in the range 3055-3095 cm^{-1}, for aromatic C-H bond, bands in the range 2815-2973 cm^{-1}, corresponding to aliphatic C-H bond, more over bands in the range 1684-1697 cm^{-1}, suggesting the presence of C=C bond, beside that a strong bands in the range 1629-1677 cm^{-1}, corresponding to carbonyl group. Additionally, compounds 5a and 5b demonstrated absorption bands at 1588 and 1597 cm^{-1}, respectively, which were attributed to the C=N bond. Furthermore, compounds 5c and 5d showed absorption bands at 3585 and 3477 cm^{-1}, corresponding to the NH_2 group. The ^{1}HNMR spectral data showed no signals corresponding to the CH_3 group, while compounds 5a-d exhibited singlets in the range δ 8.30-8.4 ppm for the NH proton. More over, compounds 5a and 5b exhibited another singlet for the NH protons of a sulfonamide group, which appears at δ 8.77 and 8.83 ppm due to the deshielding effect of the sulfonyl group. Besides that, compounds 5c and 5d demonstrated two singlet signals for NH protons at 10.17 and 10.31 ppm respectively. Additionally, compound 5a demonstrated two singlet signals at δ 2.33 and 1.92 ppm, which were attributed to CH_3 groups. Also, compound 5b showed one singlet signal at δ1.90 ppm for two CH_3 groups, Wears compound 5c demonstrated a singlet signal at δ 5.94 ppm corresponding to the NH_2 group, while compound 5d exhibited a downfield singlet signal at δ 5.83 ppm attributed to the NH_2 group.

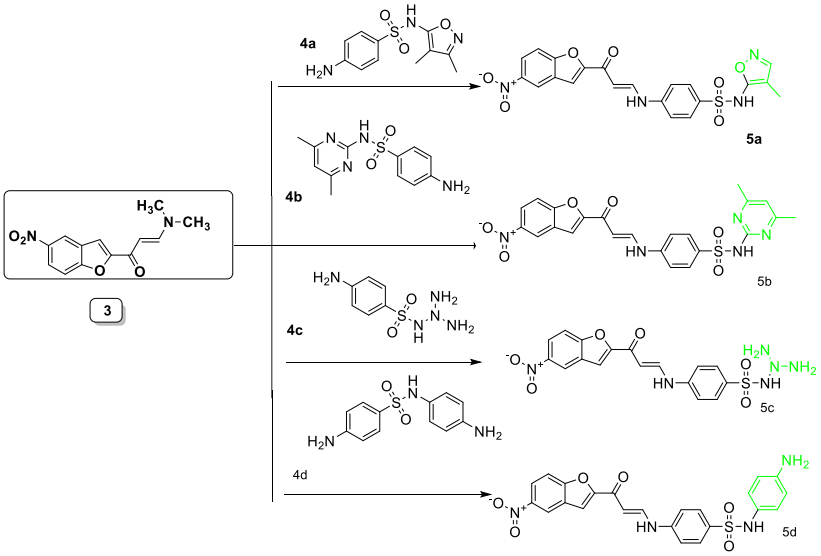

Scheme 2. Synthesis of compounds 5a-d

Received*: 03-03-2026 -* ***Accepted****: 01-05-2026 -* ***Published****: 09-05-2026*

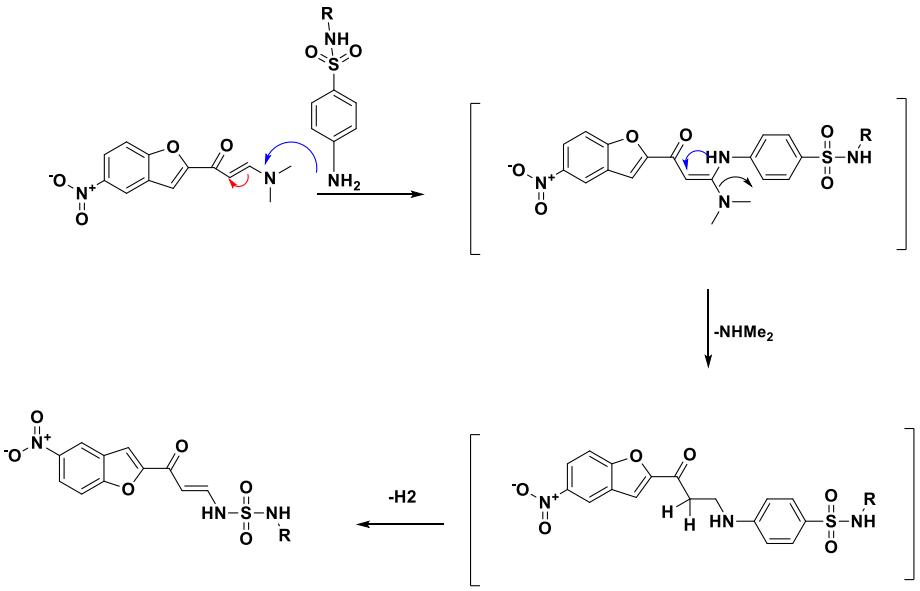

Scheme 3. Mechanism of Michael addition of amine to enaminone

In Vitro Cytotoxic Assay

Cytotoxicity activities of a novel synthesized compound, 5a-d, were performed using MTT assay against four human cell lines, WI-38, MCF-7, HePG-2, and HCT-116, doxorubicin, and sorafenib, using them as reference drugs (Table 1). show the result of the cytotoxic activity of novel synthesized compounds. Compound 5a demonstrates moderate cytotoxicity, with the lowest potency in HCT-116. With IC_{50}: 26.78±1.21 µM (WI-38), 58.52±3.3 µM (MCF-7), 62.71±3.8 µM (HePG-2), 79.33±3.7 µM (HCT-116). The increasing IC_{50} values across the cell lines suggest that this compound may be less effective against certain types of cancer. Compound 5b demonstrates the higher IC_{50} values 32.47±2.1 µM (WI-38), 65.46±3.6 µM (MCF-7), 61.62±3.6 µM (HePG-2), 87±32 µM (HCT-116). The higher IC_{50} values indicate lower potency compared to doxorubicin. Compound 5c. Notably, it shows a more favorable IC_{50} = 53.84±3.1 µM in MCF-7, suggesting it may have particular efficacy against breast cancer cells compared to the other lines with IC_{50} values 17.97±1.5 µM (WI-38), 57.24±3.4 µM (HePG-2), and 74.88±3.8 µM (HCT-116). Compound 5d exhibits the lowest IC_{50} = 311.93±2.0 µM in MCF-7, indicating strong potential against this breast cancer cell line. However, its effectiveness decreases in other lines, particularly HCT-116 with IC_{50} = 38.44±2.3 µM. The average of relative viability of cells (%) for the novel synthesized compounds 5a-d with reference drugs doxorubicin and sorafenib was summarized in (Figure 2).

Table 1. Cytotoxic activity of novel synthesized compounds 5a-d against human cell lines

No.	Comp.	In vitro Cytotoxicity IC_{50} (µM) *			
		WI-38	**MCF-7**	**HePG-2**	**HCT-116**
C1	Doxorubicin	6.72±0.5	4.17±0.2	4.50±0.2	5.23±0.3
C2	Sorafenib	10.65±0.8	7.26±0.3	9.18±0.6	5.47±0.3
1	5a	26.78±1.8	58.52±3.3	72.71±3.8	79.33±3.7
2	5b	32.47±2.1	65.46±3.6	61.62±3.6	87.32±4.3
3	5c	17.97±1.5	53.84±3.1	57.24±3.4	74.88±3.8
4	5d	75.07±3.8	31.93±2.0	29.89±1.9	38.44±2.3

**IC_{50} (µM): 1 – 10 (very strong). 11 – 20 (strong). 21 – 50 (moderate). 51 – 100 (weak) and above 100 (non-cytotoxic)*

Received*: 03-03-2026 -* ***Accepted****: 01-05-2026 -* ***Published****: 09-05-2026*

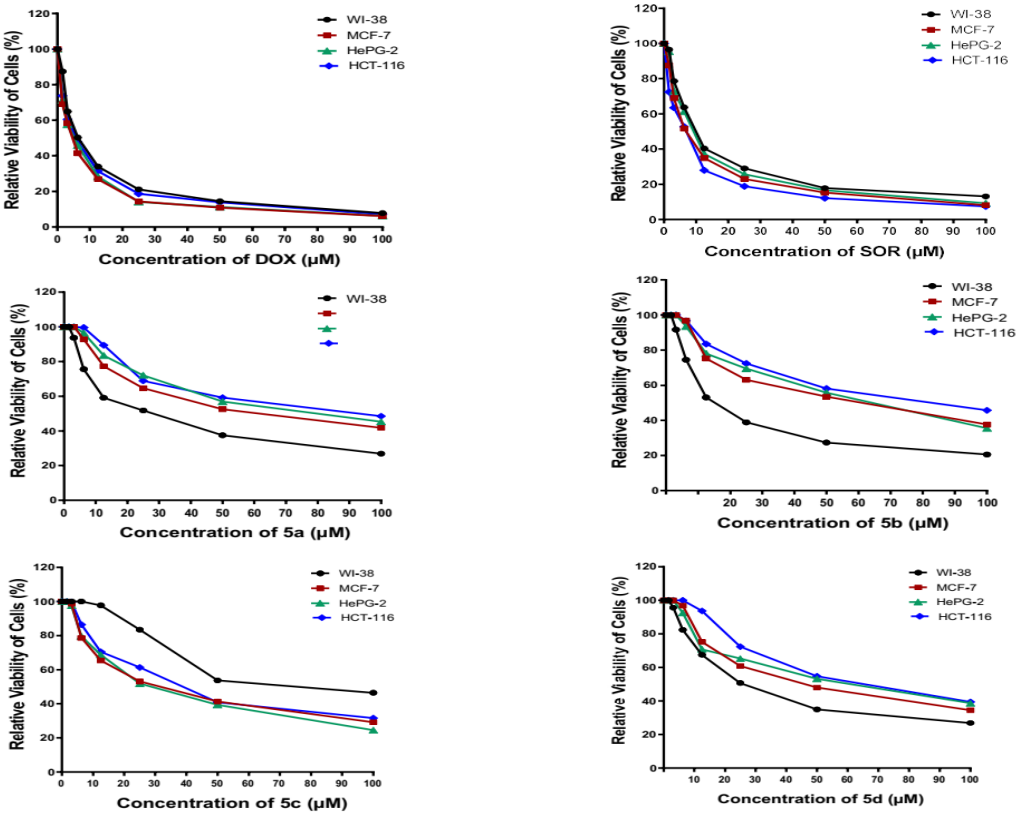

Figure 2. The relative viability of cells (%) of the novel synthesized compounds 5a-d with reference drugs doxorubicin and sorafenib

Molecular docking studies

Molecular docking was implemented for synthesized compounds and doxorubicin, which is an FDA-approved drug [36], to determine the most stable ligand-protein complex depending on the binding energy [37]. The interactions of synthesized compounds and four human cell lines: MCF-7, HePG-2, and HCT-116, and doxorubicin with the same receptors are summarized in **(**Table 2**).** The synthesized compounds demonstrated binding energy cross cell line comparison**,** compounds 5a and 5b exhibit the strongest binding energies in the MCF-7 cell line (-12.1 kcal/mol) and (-12.0 kcal/mol) respectively, indicating a high potential for effective interactions with their targets, beside that compound 5c shows moderate binding energy (-10.8 kcal/mol) suggesting a reasonable affinity but less than that of compounds 5a and 5b. While compound 5d displays the weakest binding energy in HCT116 (-9.3 kcal/mol), indicating lower affinity and potentially reduced effectiveness against this cell line. The docked compounds demonstrate crucial interactions with receptors. Compound 5a exhibited hydrogen bonds with the MCF-7 cell line at (TYR24, SER217, and TYR55) (Figure 3a, b), and with HePG-2-7 cell line at (THR137, GLN283, ASN415, GLN282, and SER80) residues, (Figure 4a, b), suggesting strong effective interactions. Compound 5b showed hydrogen bonds with MCF-7 cell line at (TYR24, SER217, TYR55, and LYS270) (Figure 3c, d) and with HePG-2 cell line at (GLN161, ASN288, ASN288, ASN415, ASN288, and HIS160) residues (Figure 4c, d) with distances indicating optimal interactions, enhancing its binding stability. Compound 5c forms hydrogen bonds with MCF-7 and HePG-2 cell lines (Figures 3-4 e, f) with moderate binding energy compared to compounds 5a and 5b. Wears Compound 5d Despite having some hydrogen bonds, the overall interaction is weaker, reflected in its higher binding energy and less favorable distances (Figure 3-6 g, h). Additionally, the docked compounds demonstrate significantly hydrophobic interactions that contribute to the binding affinity and stability of the ligand-protein complex. Compounds 5a and 5b: Engage effectively with hydrophobic residues (e.g., VAL54 and LEU219), enhancing their binding strength. These interactions are crucial for targeting cancer cells. Compound 5c, while it also engages in hydrophobic interactions, the strength may not be as pronounced as in the top compounds. Compound 5d displays weaker hydrophobic interactions, contributing to its lower binding affinity and potential efficacy.

Received*: 03-03-2026 -* ***Accepted****: 01-05-2026 -* ***Published****: 09-05-2026*

Table 2. Molecular interaction of novel synthesized benzenesulfonamide derivatives against MCF-7, HePG-2, and HC116

Compounds	Binding energy (Kcal/mol)	Amino Acid Residues Interaction			
		Hydrogen Bond	Distance	Hydrophobic	Others
MCF-7 cell line					
5a	-12.1	TYR24 SER217 TYR55	2.84137 2.62214 3.94471	TYR216, TRP227, TRP227, LEU219, LYS270, LYS270, VAL54, LEU308 and VAL54	TYR216 (Electrostatic)
5b	-12.3	TYR24 SER217 TYR55 LYS270	2.94567 2.78065 3.94679 4.17861	HIS117, TYR216, TYR24, ALA218, ALA269, LEU219, LYS270, LYS270, VAL54, LEU308	TYR216 (Electrostatic)
5c	-10.8	TYR24 ALA218 LEU219 SER221 TRP227 LYS270 LYS270 LYS270 SER221 ALA269 TYR55 TYR55 SER217	3.11461 3.28168 3.14523 3.19869 3.30405 2.96532 2.70821 2.28648 2.89317 3.66254 3.36391 3.73581 3.9378	TYR55, TYR55, LYS270	ASP50 (Electrostatic)
5d	-12.0	TYR24 ALA218 LEU219 LYS270 ALA269 TYR55 TYR55 SER217	3.02417 3.16662 3.09282 2.82973 3.74425 3.32033 3.69418 3.9008	TYR55, TYR55, LYS270, LEU219, LYS270	ASP50 (Electrostatic)
HePG-2 cell line					
5a	-11.0	THR137 GLN283 ASN415 GLN282 SER80	2.7919 2.41509 2.62939 3.0673 3.09234	4X (TRP388), PHE26, TRP412, PHE379, PHE291, PHE379	2X TRP412 (Electrostatic)
5b	-11.2	GLN161 ASN288 ASN288 ASN415 ASN288 HIS160	2.46328 2.67892 2.46621 2.64903 1.88043 2.739	4X (TRP388), HIS160, PHE26, PHE72, TRP412, ILE164	
5c	-9.9	TRP412 ASN415 ASN288 SER80 GLY408	2.69331 2.36295 1.93779 2.78519 3.04999	4X (TRP388)	GLU380 (Electrostatic)
5d	-11.2	TRP412 ASN415 GLU380 SER80 GLY138 THR137	2.70768 2.43791 2.13585 2.58517 2.70697 3.36012	PHE291, TRP388, PHE26, PHE379, VAL83, ILE404	PHE26 (Pi-Sulfur)
HC116 cell line					

Received*: 03-03-2026 -* ***Accepted****: 01-05-2026 -* ***Published****: 09-05-2026*

5a	-9.1	ASP86 GLY13	3.09019 3.43067	ILE10, LEU134, LYS89, ILE10, LYS89, ALA31, VAL18, ALA144	ASP86 (Electrostatic) 2X ASP145 (Electrostatic)
5b	-9.2	ASP86	2.61481	GLN85, ALA144, LEU298, VAL18, LEU134, ALA31, HIS84	LYS20 (Electrostatic)
5c	-8.3	LYS9 LYS9 LYS9 LYS33 LEU83	2.40153 2.86733 2.48423 3.10214 3.05492	ILE10, LEU134, VAL18, ALA31, VAL64, ALA144	ASP86 (Electrostatic)
5d	-9.3	LEU83	2.34108	ILE10, LEU134, ALA144, PHE82, PHE80, VAL18, LYS33, VAL64	PHE82 (Electrostatic)

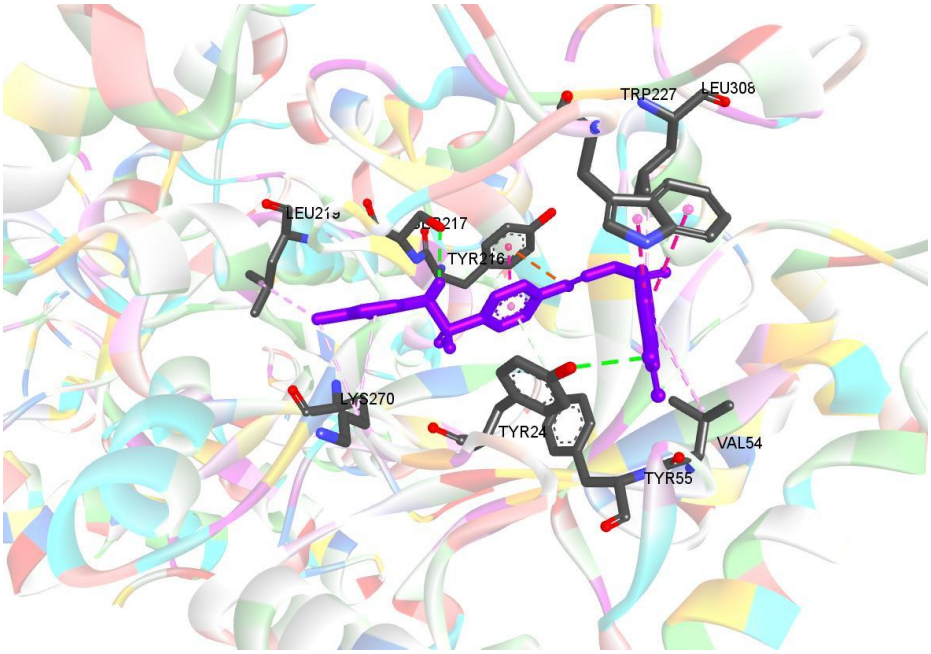

Figure 3 (a). Representation binding mode of compound 5a in the active site of protein (PDB ID:4xo6)

Received*: 03-03-2026 -* ***Accepted****: 01-05-2026 -* ***Published****: 09-05-2026*

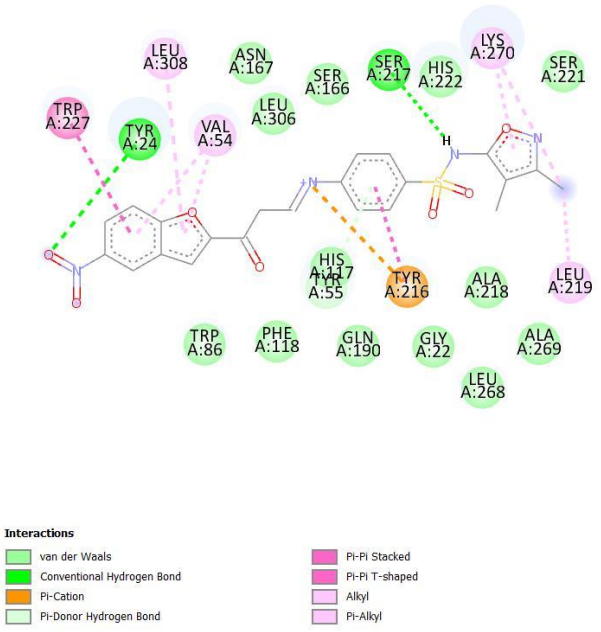

Figure 3(b). 2D diagram of interactions of compound 5a with amino acid residues

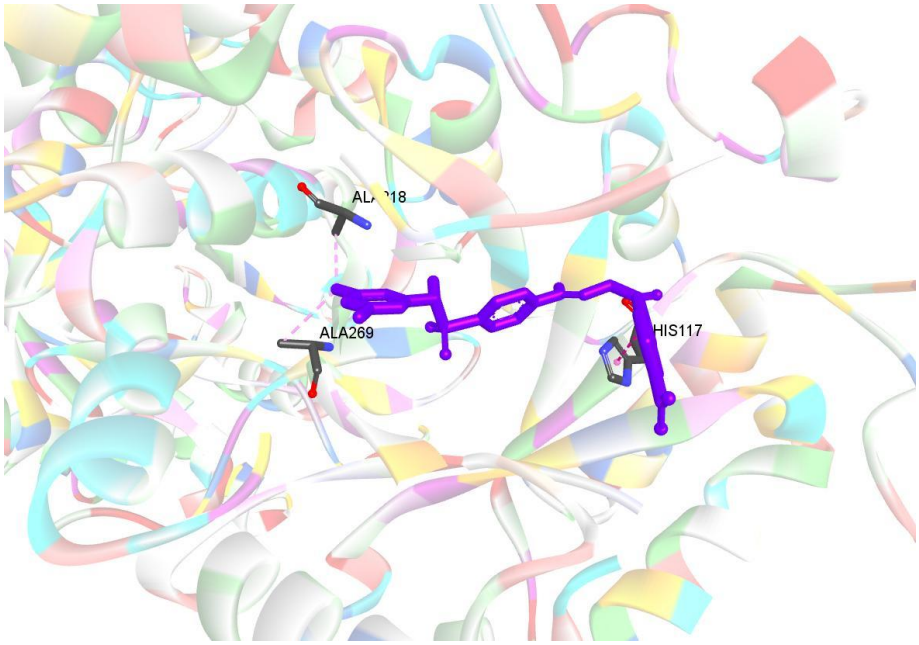

Figure 3 (c). Representation binding mode of compound 5b in the active site of protein (PDB ID:4xo6)

Received*: 03-03-2026 -* ***Accepted****: 01-05-2026 -* ***Published****: 09-05-2026*

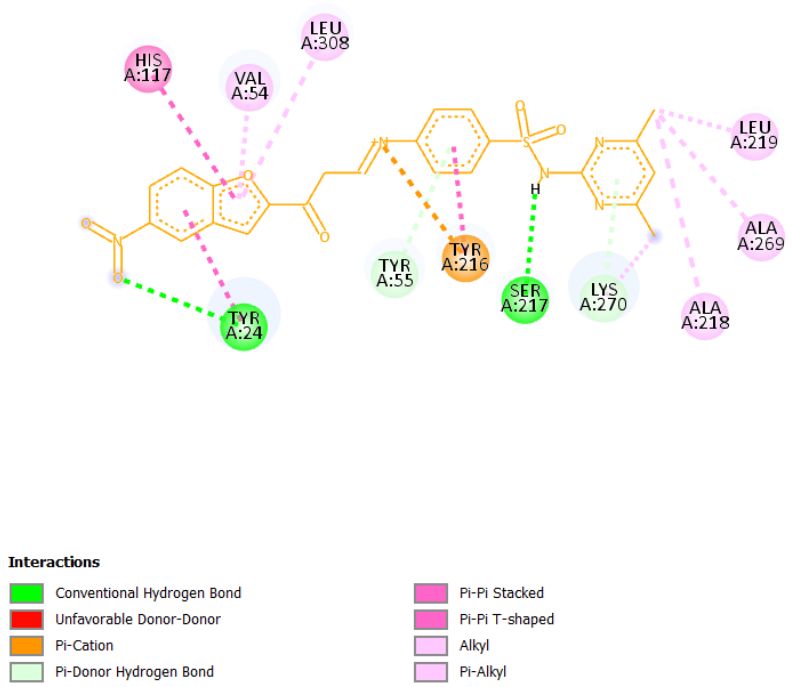

Figure 3 (d). 2D diagram of interactions of compound 5b with amino acid residues

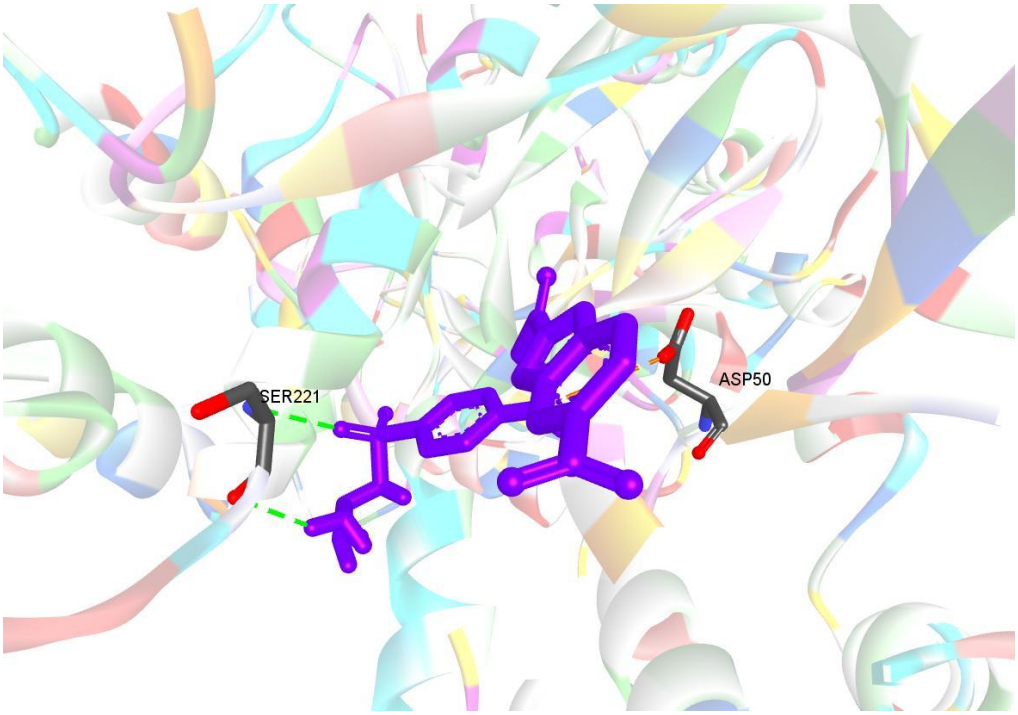

Figure 3 (e). Representation binding mode of compound 5c in the active site of protein (PDB ID:4xo6)

Received*: 03-03-2026 -* ***Accepted****: 01-05-2026 -* ***Published****: 09-05-2026*

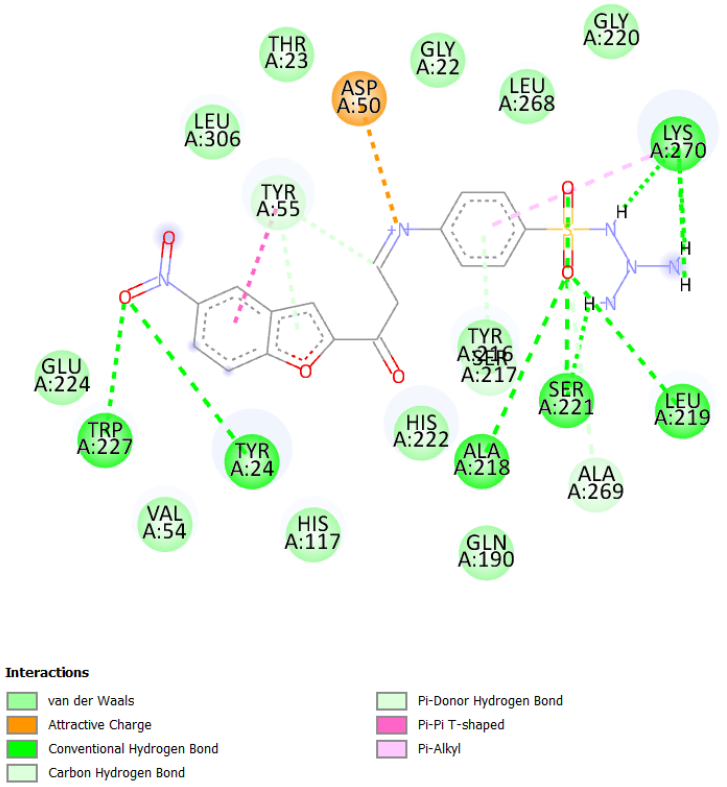

Figure 3 (f). 2D diagram of interactions of compound 5c with amino acid residues

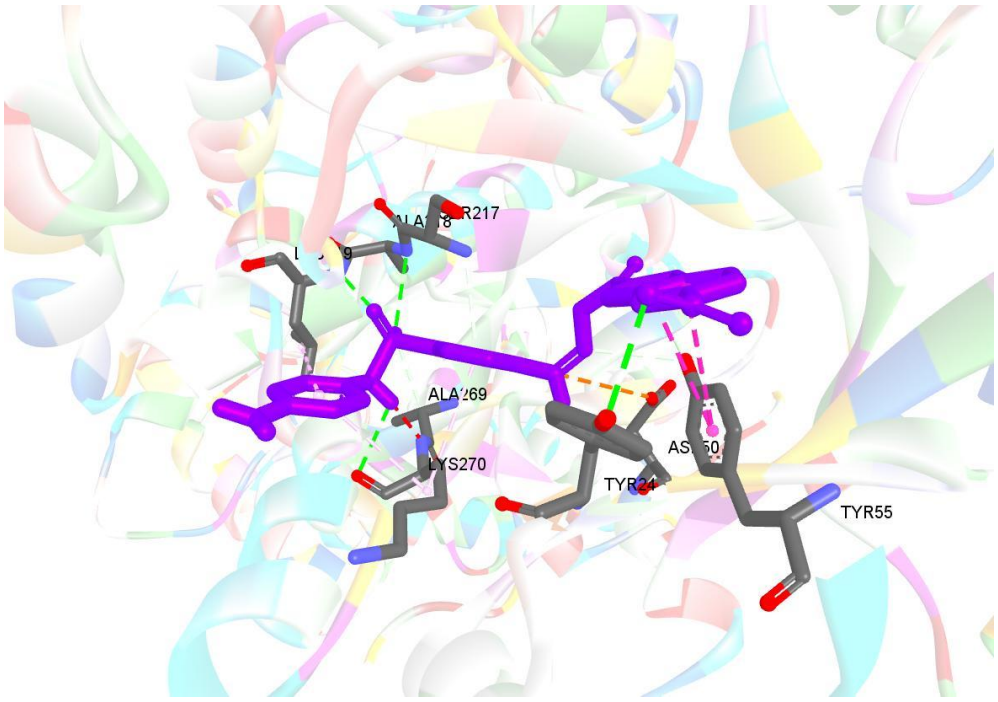

Figure 3 (g). Representation binding mode of compound 5d in the active site of protein (PDB ID:4xo6)

Received*: 03-03-2026 -* ***Accepted****: 01-05-2026 -* ***Published****: 09-05-2026*

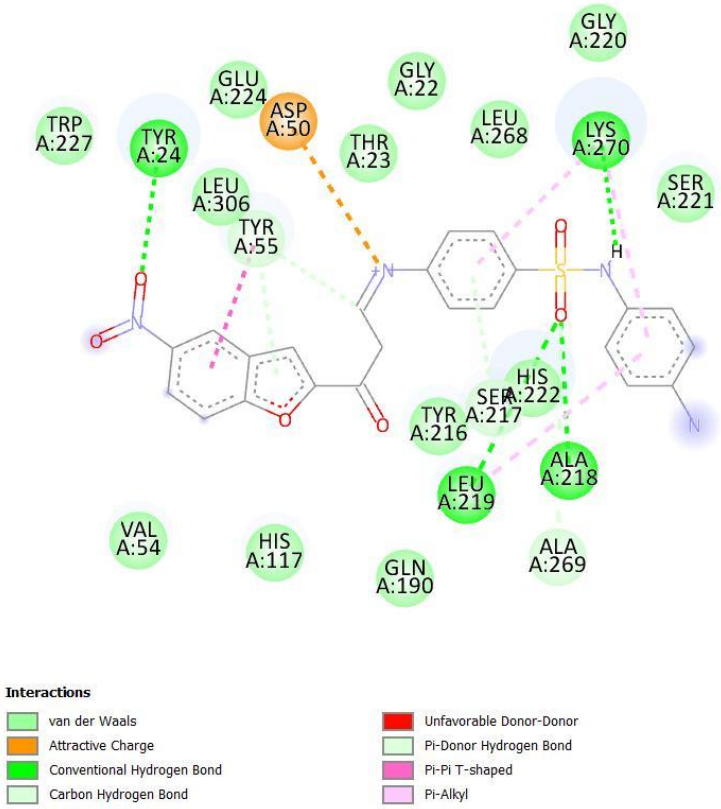

Figure 3 (h). 2D diagram of interactions of compound 5d with amino acid residues

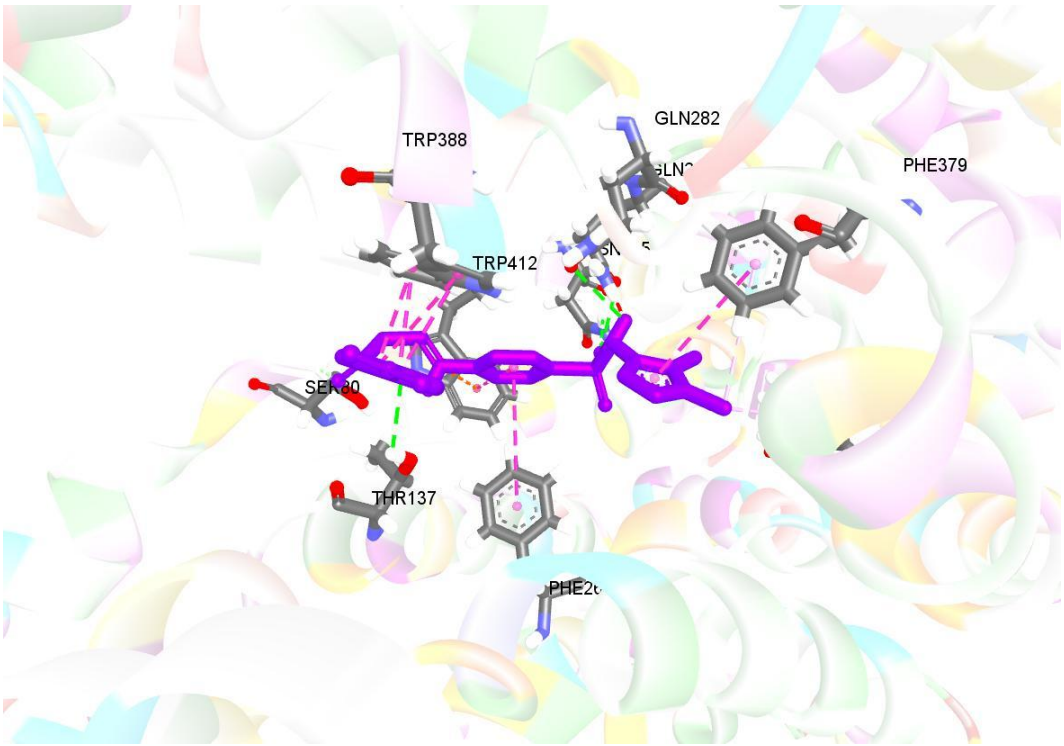

Figure 4 (a). Representation binding mode of compound 5a in the active site of protein (PDB ID: 5EQG)

Received*: 03-03-2026 -* ***Accepted****: 01-05-2026 -* ***Published****: 09-05-2026*

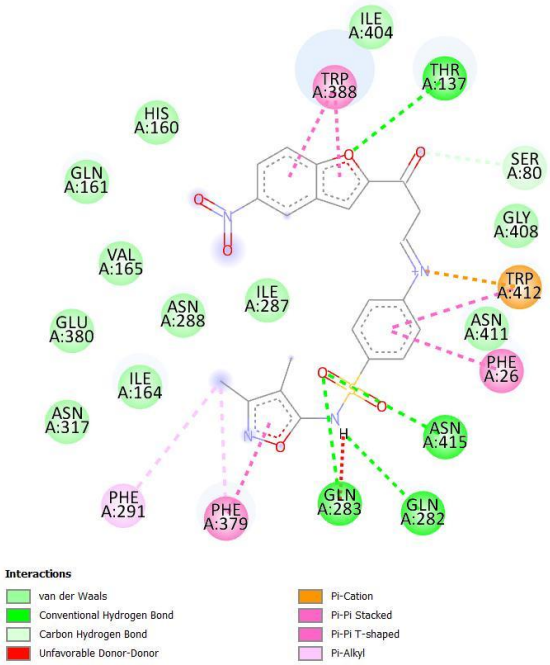

Figure 4 (b). 2D diagram of interactions of compound 5a with amino acid residues

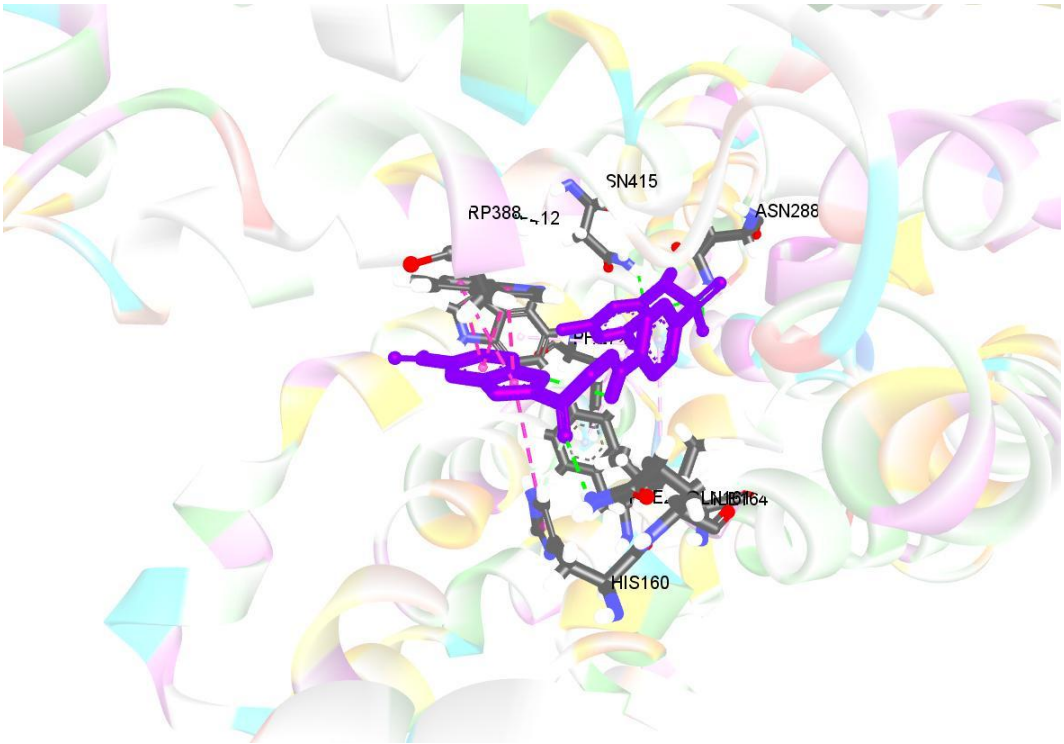

Representation binding mode of compound 5b in the active site of protein (PDB ID: 5EQG)

Received*: 03-03-2026 -* ***Accepted****: 01-05-2026 -* ***Published****: 09-05-2026*

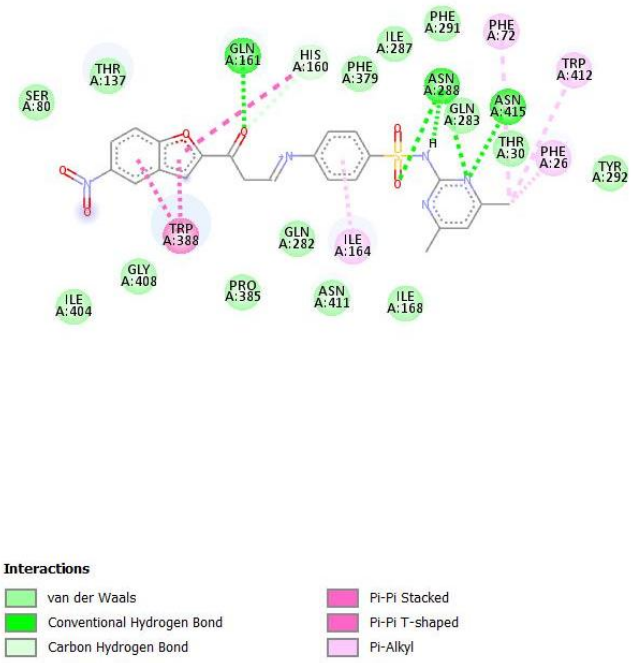

Figure 4 (d). 2D diagram of interactions of compound 5b with amino acid residues

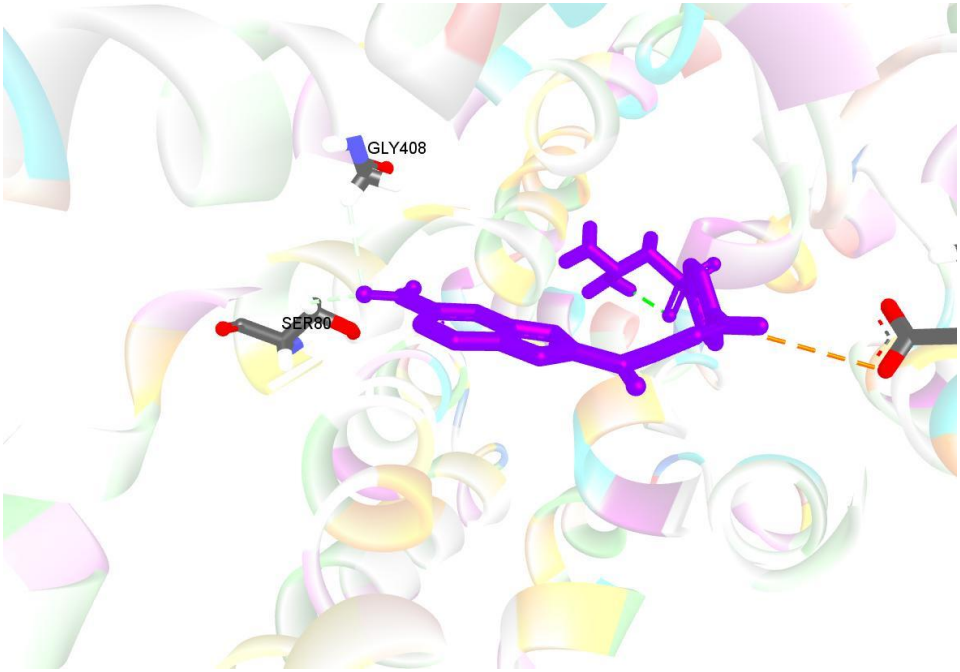

Figure 4 (e). Representation binding mode of compound 5c in the active site of protein (PDB ID: 5EQG)

Received*: 03-03-2026 -* ***Accepted****: 01-05-2026 -* ***Published****: 09-05-2026*

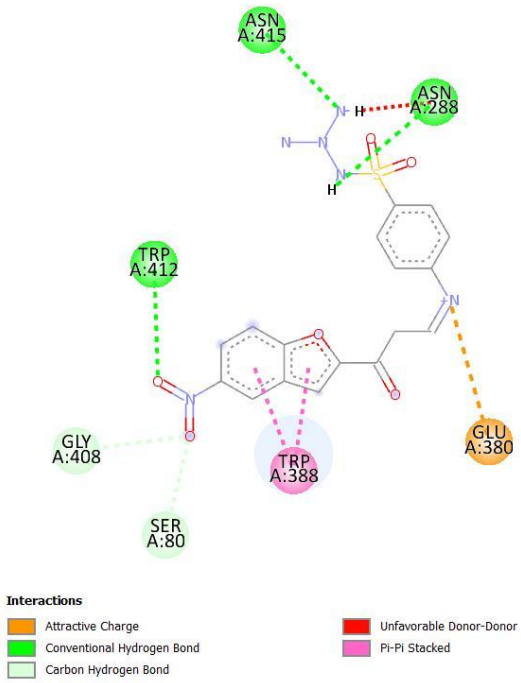

Figure 4 (f). 2D diagram of interactions of compound 5c with amino acid residues

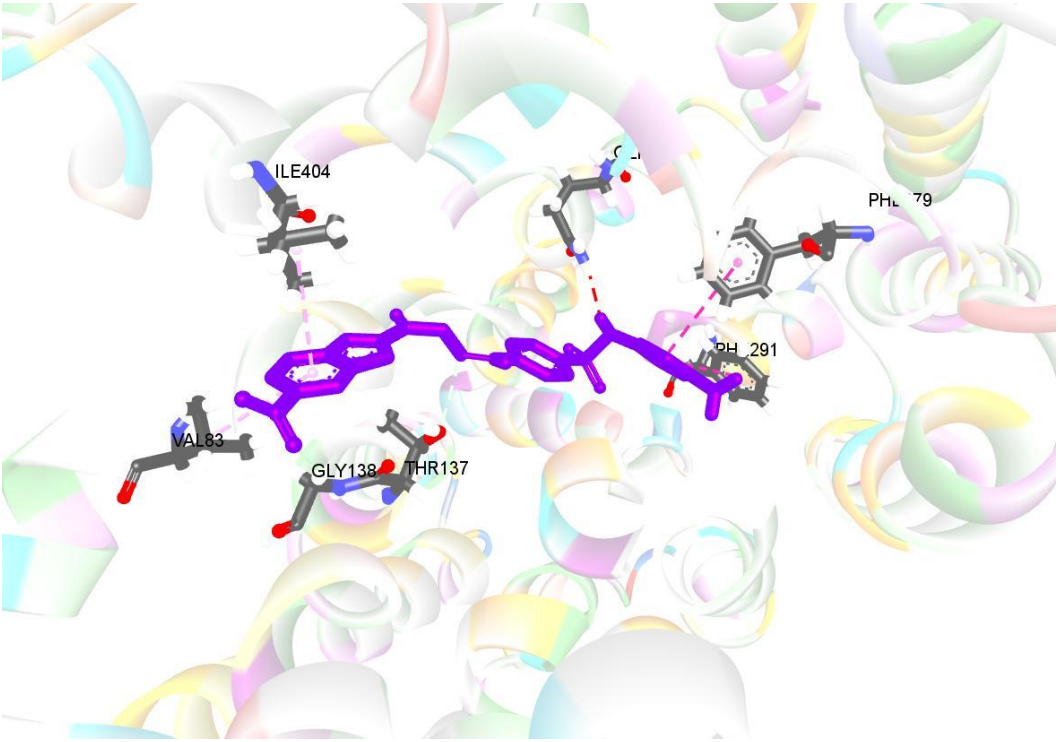

Figure 4 (g). Representation binding mode of compound 5d in the active site of protein (PDB ID: 5EQG)

Received*: 03-03-2026 -* ***Accepted****: 01-05-2026 -* ***Published****: 09-05-2026*

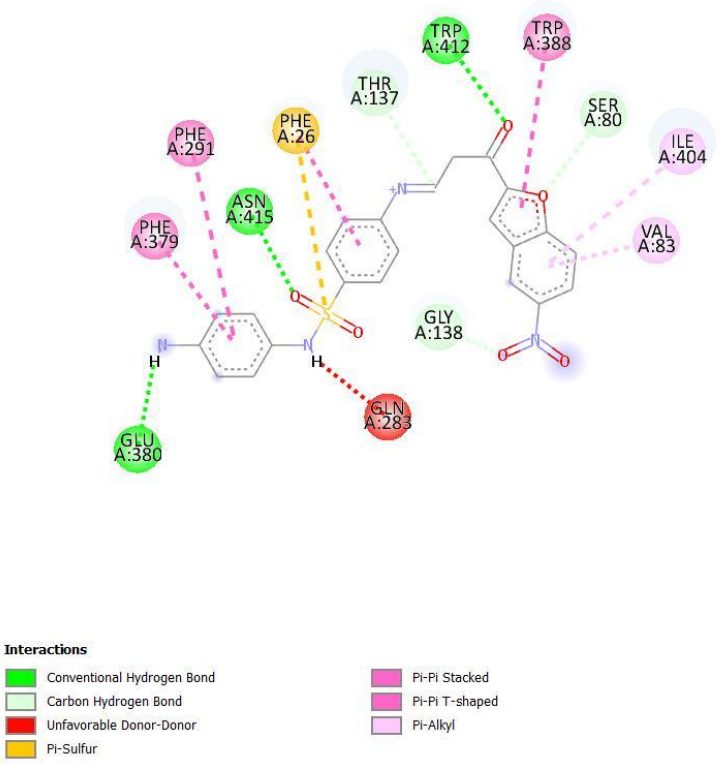

Figure 4 (h). 2D diagram of interactions of compound 5d with amino acid residues

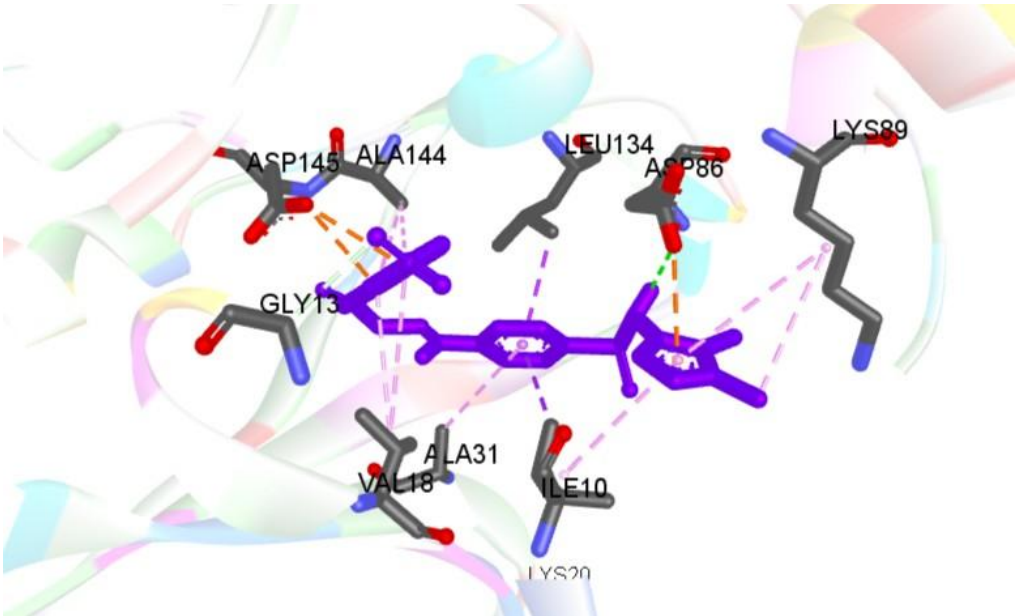

Figure 5 (a). Representation binding mode of compound 5a in the active site of protein (PDB ID: 1DI8)

Received*: 03-03-2026 -* ***Accepted****: 01-05-2026 -* ***Published****: 09-05-2026*

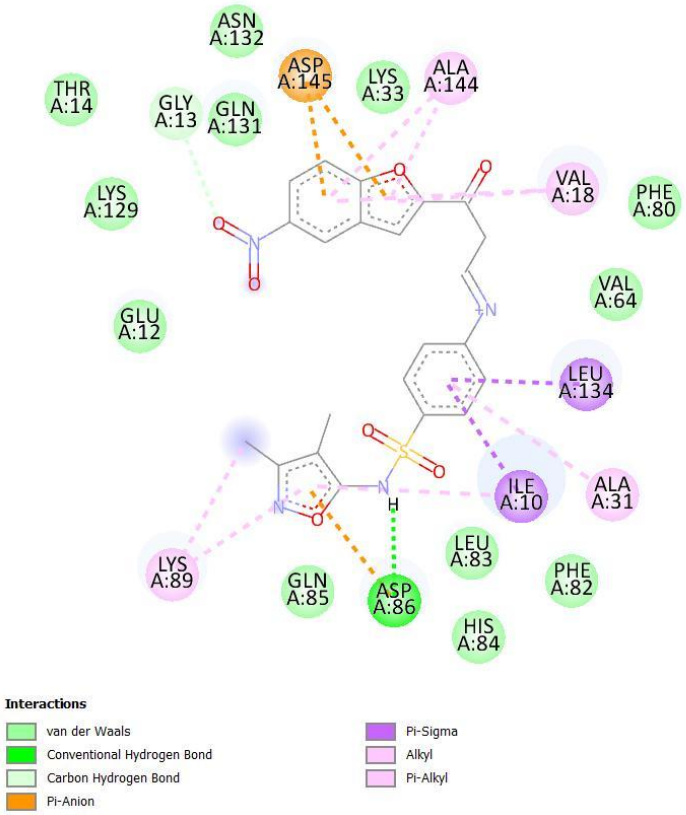

Figure 5 (b). 2D diagram of interactions of compound 5a with amino acid residues

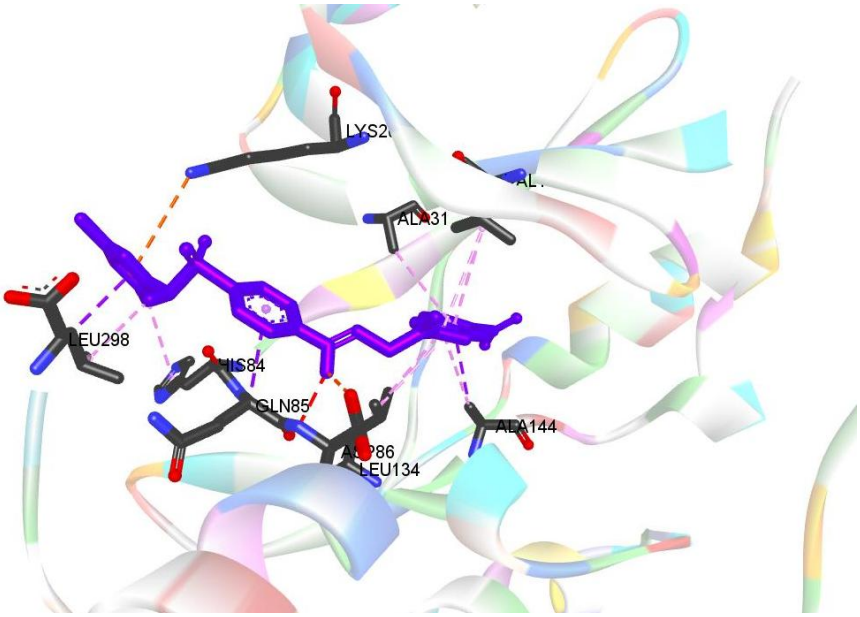

Figure 5 (c). Representation binding mode of compound 5b in the active site of protein (PDB ID: 1DI8)

Received*: 03-03-2026 -* ***Accepted****: 01-05-2026 -* ***Published****: 09-05-2026*

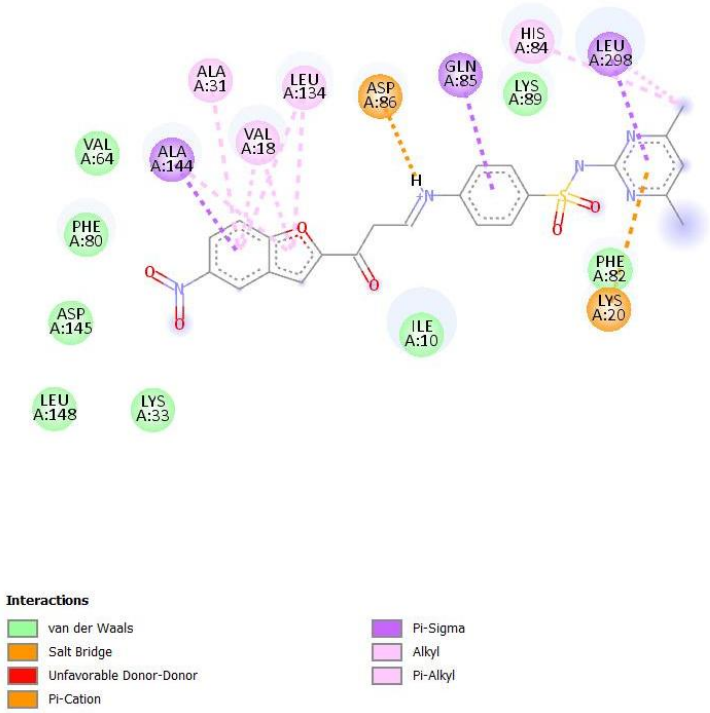

Figure 5 (d). 2D diagram of interactions of compound 5b with amino acid residues

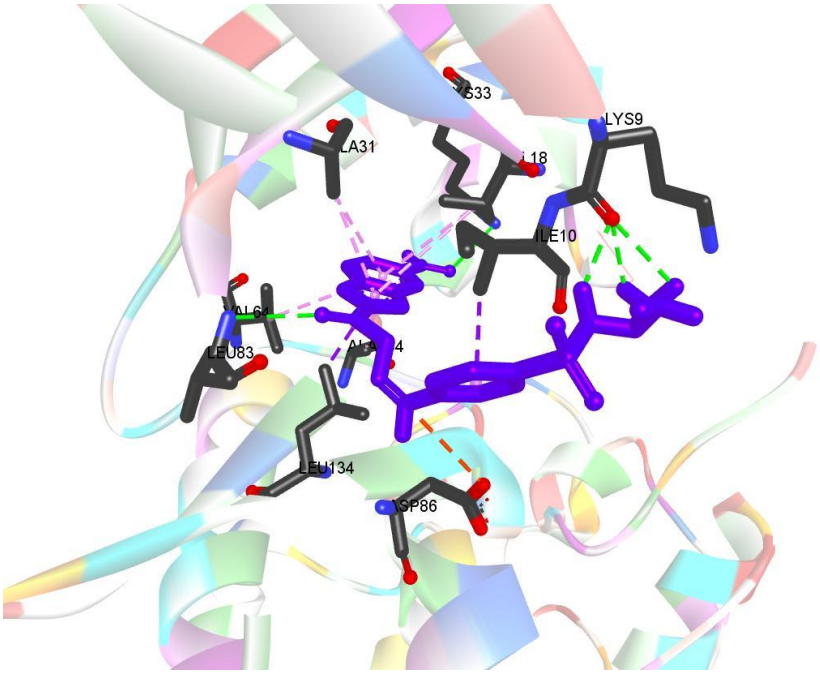

Figure 5 (e). Representation binding mode of compound 5c in the active site of protein (PDB ID: 1DI8)

Received*: 03-03-2026 -* ***Accepted****: 01-05-2026 -* ***Published****: 09-05-2026*

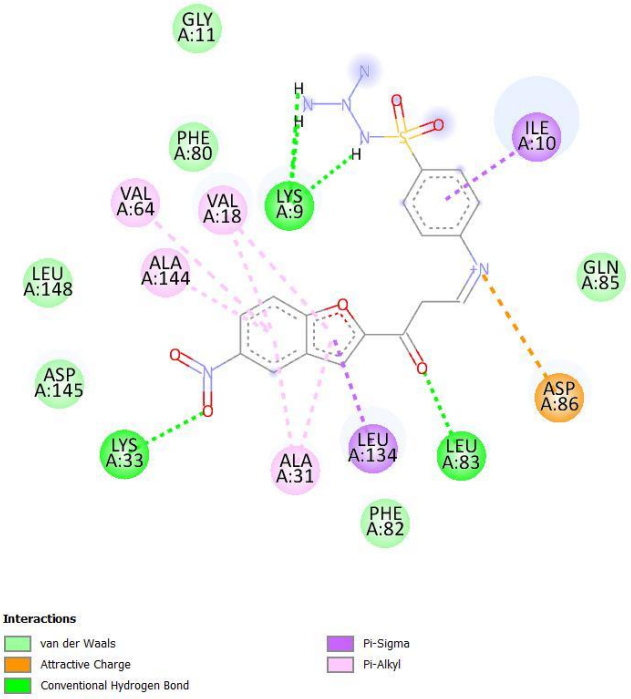

Figure 5 (f). 2D diagram of interactions of compound 5c with amino acid residues

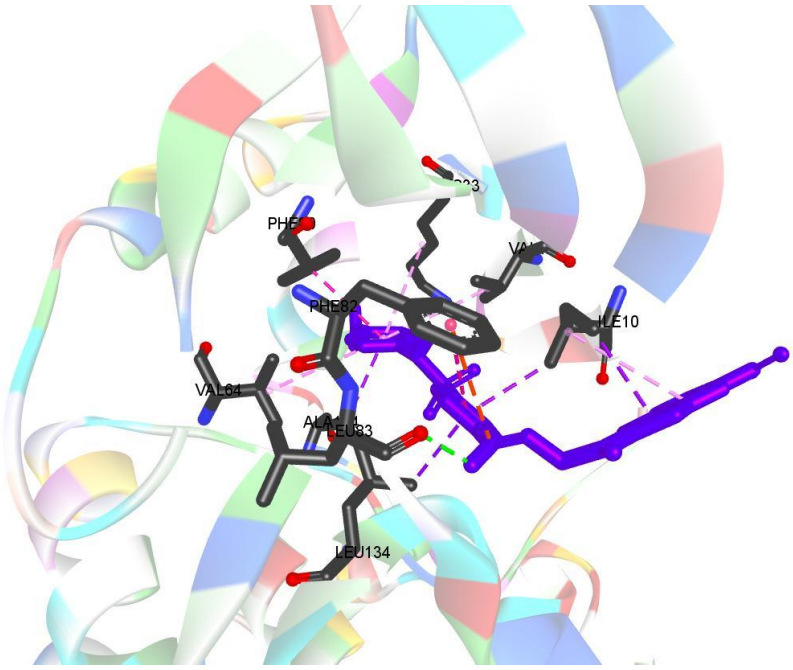

Figure 5 (g). Representation binding mode of compound 5d in the active site of protein (PDB ID: 1DI8)

Received*: 03-03-2026 -* ***Accepted****: 01-05-2026 -* ***Published****: 09-05-2026*

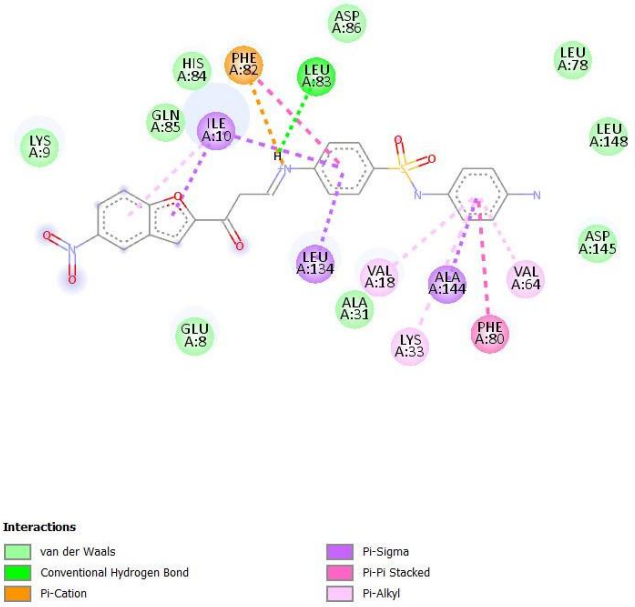

Figure 5 (h). 2D diagram of interactions of compound 5d with amino acid residues

Conclusion

The varying IC_{50} values across compounds and cell lines suggest that each compound has a unique profile of cytotoxicity, highlighting the importance of specificity in cancer treatment. Compounds 5a and 5d may warrant further investigation, particularly in the context of MCF-7, where they showed promising results. The trends in IC_{50} values also suggest an opportunity to modify the chemical structure of these compounds to enhance their potency and reduce toxicity. The effectiveness of the compounds varies significantly across different cancer cell lines, highlighting the importance of the tumor microenvironment in therapeutic outcomes. MCF-7: Compounds 5a and 5b show strong binding interactions, indicating high potential for effective treatment in breast cancer. HePG-2: Compound 5b presents promising interactions, suggesting it may be particularly effective against liver cancer. HCT116: Compound 5d shows reduced binding energy and weaker interactions, suggesting it may not be as effective against colon cancer compared to others.

References

1. Abraham J. Cancer Res. 1966;26:123–145.
2. Acar Selçuki N, Coşkun KA, Yıldız M. Eur J Med Chem. 2020;185:111825.
3. Siegel R, Ma J, Zou Z, Jemal A. CA Cancer J Clin. 2014;64:9–29.
4. Yu J, Liu Y, Gong Z, Zhang S, Guo C, Li X, et al. Oncotarget. 2014;5:10718–10732.
5. Bourgeois Daigneault S, Roy DG, Aitken AS, El Sayes N, Martin NT, Varette O, et al. Mol Ther. 2016;24:1202–1214.
6. Kreike B, van Kouwenhove M, Horlings H, Weigelt B, Peterse H, Bartelink H, et al. Breast Cancer Res. 2007;9:R65.
7. World Health Organization. Global Cancer Observatory. 2021.
8. Prestinaci F, Pezzotti P, Pantosti A. Lancet Infect Dis. 2015;5:1170–1179.
9. Ventola CL. P&T. 2015;40:277–283.
10. Supuran CT. J Enzyme Inhib Med Chem. 2017;32:902–913.
11. Supuran CT, Scozzafava A, Casini A. Med Res Rev. 2003;23:535–558.
12. Boufas W, Dupont N, Berredjem M, Berrée F, Carboni B, Roisnel T, et al. Eur J Med Chem. 2014;76:165–174.
13. Tacic A, Nikolic V, Nikolic L, Savic I. Molecules. 2017;22:562.
14. Guianvarc'h D, Duca M, Boukarim C, Kraus-Berthier L, Léonce S, Pfeiffer B, et al. J Med Chem. 2004;47:2365–2374.
15. Root DE, Braun CR, VerPlank L, Ferraiolo P, Prajapati S, Campbell JE, et al. Cell Chem Biol. 2018;25:1015–1024.
16. Giles AJ, Hutchinson MKN, Sonnemann HM, Jung J, Fecci PE, Ratnam NM, et al. Nat Commun. 2019;10:4011.
17. Shah RR, Stonier PD. Ther Adv Drug Saf. 2018;9:559–588.
18. Hehui F, Yujie L, Xiaoyan W, Xiaoyan Z, Zhigang L. Environ Sci Pollut Res. 2021;28:4329–4340.
19. Alam MJ, Alam O, Naim MJ, Nawaz F, Manaithiya A, Imran M, et al. Eur J Med Chem. 2023;245:114898.
20. Janprasert J, Satitpatipan V, Kasisit J, Reutrakul V, Tuchinda P. Phytochemistry. 1992;31:2193–2196.
21. Lee JS, Miyashiro H, Nakamura N, Hattori M. Chem Pharm Bull. 1998;46:684–685.
22. Dawood KM. RSC Adv. 2019;9:41259–41293.
23. Miao Y, Liu J, Liu X, Han B, Yuan H. Bioorg Med Chem Lett. 2019;29:126683.
24. Sharma P, Kumar A, Upadhyay A, Sahu V, Singh J, Mishra A. Bioorg Chem. 2022;118:105485.
25. Sung H, Ferlay J, Siegel RL, Laversanne M, Soerjomataram I, Jemal A, et al. CA Cancer J Clin. 2021;71:209–249.
26. Chen Y, Zhang W, Huang Y, Gao F, Fang X. Eur J Med Chem. 2023;245:114900.
27. Li H, Wang Z, Zhang Y, Li X, Yu J, Wu J, et al. Bioorg Chem. 2023;130:106234.
28. Wu TY, Cho TY, Lu CK, Liou JP, Chen MC. Sci Rep. 2017;7:12406.

Received*: 03-03-2026 -* ***Accepted****: 01-05-2026 -* ***Published****: 09-05-2026*

29. Ghorab MM, Alsaid MS, Soliman AM, Ragab FA. J Enzyme Inhib Med Chem. 2017;32:893–907.
30. Żołnowska B, Sławiński J, Brzozowski Z, et al. Int J Mol Sci. 2018;19:1482.
31. Qiu Q, Zhu J, Chen Q, et al. Bioorg Chem. 2019;90:103083.
32. Gregorić T, Sedić M, Grbčić P, et al. Eur J Med Chem. 2017;125:1247–1267.
33. Gholampour M, Ranjbar S, Edraki N, Mohabbati M, Firuzi O, Khoshneviszadeh M. Bioorg Chem. 2019;88:102967.
34. Zhao YL, Wang Y, Wulff WD. Synlett. 2007;19:3063–3066.
35. Pathak U, Pandey LK, Tank R. J Heterocycl Chem. 2010;47:1353–1358.
36. Cortazar P, Justice R, Johnson J, Sridhara R, Keegan P, Pazdur R. J Clin Oncol. 2012;30:1705–1711.
37. Das DR, Kumar D, Kumar P, Dash BP. J Appl Biol Biotechnol. 2020;8:105–116.
38. Janowska S, Khylyuk D, Bielawska A. Molecules. 2022;27:1–23.
39. Arechabala B, Coiffard C, Rivalland P, Coiffard LJM, De Roeck-Holtzhauer Y. J Appl Toxicol. 1999;19:163–165.
40. Mitra I, Mukherjee S, Reddy VB, Venkata PB. RSC Adv. 2016;6:76600–76613.
41. Gornowicz A, Szymanowska A, Mojzych M, Bielawski K, Bielawska A. Int J Mol Sci. 2020;21:1–18.

Received*: 03-03-2026 -* ***Accepted****: 01-05-2026 -* ***Published****: 09-05-2026*